

Spin relaxation by dipolar coupling: From motional narrowing to the rigid limit

Alexander A. Nevzorov and Jack H. Freed^{a)}

Department of Chemistry and Chemical Biology, Cornell University, Ithaca, New York 14853

(Received 25 August 1999; accepted 22 October 1999)

A coupled system of two molecules bearing spins of 1/2, which are allowed to diffuse relative to each other, is considered. By using a symmetry-adapted basis operator set, the overall density matrix equation is decoupled into two equations for the time-resolved isochromat components, the sum of which yields the observed signal. The appropriate stochastic Liouville equation is solved by a combination of eigenfunction expansion and finite-differences for the angular and radial relative motions, respectively. A full range of spectra from classic Pake patterns in the rigid limit to motionally narrowed Lorentzians is recovered. As an extension of the above approach, the solid-echo experiment is described in terms of the ensemble-averaged isochromats. Homogeneous transverse relaxation times (T_2) as a function of the translational diffusion coefficient (D_T) are obtained from simulating SECSY (spin-echo correlation spectroscopy) signals, which show distinct T_2 minima vs D_T . The present method of separating the quantum and stochastic classical variables constitutes a useful approach for treating multiquantum statistical systems, and it can be generalized to an arbitrary number of spins as shown in a companion paper. In the present study we obtained the usual linear dependence of T_2 on D_T in the motional narrowing (or Redfield) limit, whereas in the slow motional regime a $D_T^{-1/2}$ dependence is observed, consistent with studies of rotational diffusion. Varying the distance of maximum separation between the two spins (r_{\max}) has virtually no effect on the location of the T_2 minimum with respect to D_T , implying that the onset of slow motion is essentially independent of r_{\max} . © 2000 American Institute of Physics. [S0021-9606(00)02803-8]

I. INTRODUCTION

General solutions to the problem of spin relaxation from the motional narrowing regime, where Bloch–Wangsness–Redfield theory applies,^{1,2} to the rigid limit have been available for some time.^{3–6} The most powerful approach is based on solving the stochastic Liouville equation (SLE). This approach has been applied to cases of slow-tumbling in ESR (electron spin resonance) and NMR (nuclear magnetic resonance),^{5,6} as well as to chemically induced electronic and nuclear spin polarization (CIDEP and CIDNP) involving relative translational diffusion of radical pairs.^{4,7} Another useful approach, but more difficult to execute numerically is the method of cumulant expansions.⁸ Freed⁹ has applied this method to ESR, and recently Brüschweiler¹⁰ to NMR using a sixth-order expansion. One case that has not yet been adequately analyzed is that of spin relaxation by dipolar interaction between two spin-bearing molecules engaged in relative translational diffusion. In the motional narrowing regime the solutions are well-known.^{1,11–13} In fact, they are usually extended to the interaction of many spin-bearing molecules in a dilute nonviscous solution by simple additivity of the pairwise interactions.^{1,12,13}

In this paper and a companion paper,¹⁴ hereinafter referred to as Paper I and Paper II, respectively, we address the issue of dipolar relaxation between spin bearing molecules in

dilute solution that are diffusing relative to one another, in which we bridge the gap between the motional narrowing regime and the rigid limit. In this paper, we just consider two spin-bearing molecules in relative motion, and in Paper II we address the many-body problem. While the first case of two spin-bearing molecules can be solved by direct application of the SLE, the many-body problem is inherently much more complex, requiring a more sophisticated procedure in order to derive a soluble form of the appropriate SLE. For purposes of clarity of exposition, we introduce some of the formal procedures that will be needed in Paper II in the present paper, where the details are much simpler. Whereas this makes the derivation in this paper somewhat more involved, we believe it helps to set the stage for Paper II, wherein the present two-spin analysis will be extended to the thermodynamic limit (i.e., for an infinitely large number of spins N and macroscopic volume, V , but with concentration $C \equiv N/V$ remaining finite). The present study in Paper I for just two spins does not simply lend itself to the thermodynamic limit.

The relatively simple problem of two diffusing spin-bearing molecules is still of practical interest. In particular, by restricting the relative translational diffusion to an inner radial limit, $r_{\min}=d$, and an outer one r_{\max} , one achieves a simple model for a flexible biradical in which radical moieties at either end are tethered to restrict their maximum separation to r_{\max} . Such models have previously been studied in the context of CIDNP and CIDEP, where, however,

^{a)}Electronic mail: jhf@msc.cornell.edu

the primary spin-dependent interaction of interest was an isotropic exchange interaction.^{15,16} Here we are interested in magnetic resonance line shapes, as well as FID (free-induction delay) and spin echo experiments, for the case where we restrict the primary spin-spin interaction to the intermolecular dipolar interaction, (although we comment on how the analysis may be modified in order to include the exchange interaction). This is a topic of growing interest in the ESR study of bilabeled macromolecules, such as proteins¹⁷ and polymers.¹⁸

In the motional narrowing regime, the line broadening is homogeneous, and it will not be refocused in an echo. In the rigid limit the broadening is inhomogeneous, and for the case of dipolar interaction between two like spins it gives rise to classical Pake patterns. This broadening may be refocused by a solid echo.² In order to clarify the changing behavior from homogeneous to inhomogeneous broadening we also obtain the solid echoes in the slow motional regime and compare them with the FID's. We further consider the role of the radial separation on whether the dipolar interaction is completely or only partially averaged.

This paper is organized as follows. In Sec. II we develop the expressions needed for the system of two interacting spins. Here we expand the density matrix in the "symmetry-adapted" basis set of eigenoperators originally introduced by Banwell and Primas,¹⁹ and we consider the coupled equations of motion for the coefficients of the expansion. Expansion of the overall density matrix into an eigenoperator basis allows one to separate the quantum variables of the system from the stochastic classical variables, and then allows one to follow more easily the multiple-coherence pathways even in the presence of relaxation. The FID signal is then written as a time-ordered ensemble average over the sum of the two isochromat components. In Sec. III the formal relationship of this result to the appropriate SLE is described, and the method of solution of the SLE is given. It involves a combination of eigenfunction expansions for the orientational part of \mathbf{r} and finite-differences for the magnitude, r , in a manner related to the methods of Hwang & Freed¹² for dipolar interactions in the motional narrowing regime and Zientara & Freed²⁰ for CIDEP with an anisotropic exchange interaction. In Sec. IV we derive expressions for spin-echo experiments using the solid echo as the primary example. In Sec. V we describe the results of model simulations of line shapes, FID's, and solid echoes, and in Sec. VI we summarize our conclusions.

II. EQUATIONS FOR SPIN-ISOCROMAT COMPONENTS WITHIN THE EIGENOPERATOR BASIS: THE FID SIGNAL

For a system of two interacting spins, one can write the spin Hamiltonian as a sum of the time-independent Zeeman part and the time-dependent perturbation due to the dipolar interaction between the spins. That is

$$H = H_0 + H^{(1,2)}, \quad (2.1)$$

where the unperturbed Zeeman Hamiltonian H_0 in the rotating frame is

$$H_{0,R} = \Delta\Omega_1 I_z^{(1)} + \Delta\Omega_2 I_z^{(2)}, \quad (2.2a)$$

where $\Delta\Omega_i$ is the resonant frequency offset for the i th spin with respect to the oscillating rf (radio frequency) magnetic field ω_{rf} , i.e., $\Delta\Omega_i = \Omega_i - \omega_{rf}$. Eq. (2.2a) for the case of like spins becomes

$$H_{0,R} = \Delta\Omega [I_z^{(1)} + I_z^{(2)}]. \quad (2.2b)$$

Here, we consider the high-field approximation and retain only the secular terms of the dipolar interaction Hamiltonian, namely

$$H^{(1,2)} = H_R^{(1,2)} = \chi \frac{Y_0^{(2)}(\theta, \phi)}{r^3} \left[I_z^{(1)} I_z^{(2)} - \frac{1}{4} (I_+^{(1)} I_-^{(2)} + I_-^{(1)} I_+^{(2)}) \right], \quad (2.3)$$

where $\chi \equiv \sqrt{(16\pi/5)} \gamma^2 \hbar$ is the coupling constant, r is the distance between the spins, $Y_0^{(2)}(\theta, \phi)$ is the spherical harmonic of rank two and order zero, and the polar angles θ and ϕ describe the orientation of the radial vector \mathbf{r} connecting the two spins in the lab frame, in which the dc magnetic field is taken along the z axis. The equation of motion for the density matrix in the rotating frame, $\rho_R(\mathbf{r}; t)$ is

$$\frac{\partial \rho_R(\mathbf{r}; t)}{\partial t} = -i [H_{0,R} + H_R^{(1,2)}, \rho_R(\mathbf{r}; t)]. \quad (2.4)$$

One can write the free-induction decay (FID) signal in terms of an ensemble-average over the classical random variable \mathbf{r} , denoted by angular brackets, as

$$\begin{aligned} G(t) \propto \langle M_x(\mathbf{r}; t) \rangle &= \text{Tr}[(I_x^{(1)} + I_x^{(2)}) \langle \rho_R(\mathbf{r}; t) \rangle] \\ &= \text{Tr}[\frac{1}{2}(I_+^{(1)} + I_+^{(2)}) \langle \rho_R(\mathbf{r}; t) \rangle] \\ &\quad + \text{Tr}[\frac{1}{2}(I_-^{(1)} + I_-^{(2)}) \langle \rho_R(\mathbf{r}; t) \rangle]. \end{aligned} \quad (2.5)$$

Thus, we seek the solution of the ensemble-averaged density matrix, $\langle \rho_R(\mathbf{r}; t) \rangle$.

For a system of two spins of 1/2, one can construct sixteen eigenoperators E_ϵ of the superoperator form of the unperturbed Hamiltonian H_0 , which Banwell and Primas call the symmetry-adapted basis set,¹⁹ such that

$$H_D^\dagger E_\epsilon \equiv [H_0, E_\epsilon] = \mu \Omega E_\epsilon. \quad (2.6)$$

These eigenoperators are linearly independent and orthonormal with respect to the Frobenius trace metric, viz.

$$(E_\epsilon, E_{\epsilon'}) \equiv \text{Tr}(E_\epsilon^\dagger E_{\epsilon'}) = \delta_{\epsilon\epsilon'}. \quad (2.7)$$

However, to calculate the FID signal, we need to consider, following Banwell and Primas, only those eight that have nonzero Frobenius projections [cf. Eq. (2.7)] on operators $I_+^{(1)}$, $I_+^{(2)}$, $I_-^{(1)}$, and $I_-^{(2)}$, cf. Eq. (2.5). These eigenoperators all have $\mu = \pm 1$ and are given by the following direct products of single-spin operators:

$$\begin{aligned} E_1 &= I_+^{(1)} I_\alpha^{(2)}, & E_3 &= I_+^{(1)} I_\beta^{(2)}, \\ E_2 &= I_+^{(2)} I_\alpha^{(1)}, & E_4 &= I_+^{(2)} I_\beta^{(1)}, \end{aligned} \quad (2.8a)$$

corresponding to $\mu=+1$, and

$$E_5 = I_-^{(1)} I_\alpha^{(2)}, \quad E_7 = I_-^{(1)} I_\beta^{(2)}, \quad (2.8b)$$

$$E_6 = I_-^{(2)} I_\alpha^{(1)}, \quad E_8 = I_-^{(2)} I_\beta^{(1)},$$

corresponding to $\mu=-1$, where

$$I_+ = \begin{pmatrix} 0 & 1 \\ 0 & 0 \end{pmatrix}, \quad I_- = \begin{pmatrix} 0 & 0 \\ 1 & 0 \end{pmatrix}, \quad (2.9)$$

$$I_\alpha \equiv \frac{1}{2} \mathbf{1} + I_z = \begin{pmatrix} 1 & 0 \\ 0 & 0 \end{pmatrix}, \quad I_\beta \equiv \frac{1}{2} \mathbf{1} - I_z = \begin{pmatrix} 0 & 0 \\ 0 & 1 \end{pmatrix},$$

which are easily related to the Pauli spin matrices. As follows from Eq. (2.5) and their trace properties, the group of operators having $\mu=+1$ can be considered separately from those with $\mu=-1$ for the purposes of finding the FID signal. Therefore, we decompose the relevant subspace of the overall density matrix into two linear combinations of the four eigenoperators

$$\rho_R(\mathbf{r};t) = \sum_{\epsilon=-a}^b g_\epsilon(\mathbf{r};t) E_\epsilon, \quad (2.10)$$

where either $a=1$ and $b=4$ or else $a=5$ and $b=8$, and the coefficients $g_\epsilon(\mathbf{r};t)$ are functions of time. Substituting Eq. (2.10) into the equation for the density matrix (2.4), and calculating the commutators of E_ϵ with $H^{(1,2)}$, one obtains the following system of equations for the first four components $g_\epsilon(\mathbf{r};t)$ in the rotating frame, after making use of the orthonormality of the eigenoperators, Eq. (2.7)

$$\frac{\partial g_1(\mathbf{r};t)}{\partial t} = -i\Delta\Omega_1 g_1(\mathbf{r};t) - i\chi F(\mathbf{r};t) \left[\frac{1}{2} g_1(\mathbf{r};t) + \frac{1}{4} g_2(\mathbf{r};t) \right], \quad (2.11a)$$

$$\frac{\partial g_2(\mathbf{r};t)}{\partial t} = -i\Delta\Omega_2 g_2(\mathbf{r};t) - i\chi F(\mathbf{r};t) \left[\frac{1}{4} g_1(\mathbf{r};t) + \frac{1}{2} g_2(\mathbf{r};t) \right], \quad (2.11b)$$

$$\begin{aligned} \frac{\partial g_3(\mathbf{r};t)}{\partial t} &= -i\Delta\Omega_1 g_3(\mathbf{r};t) - i\chi F(\mathbf{r};t) \left[-\frac{1}{2} g_3(\mathbf{r};t) - \frac{1}{4} g_4(\mathbf{r};t) \right], \\ & \quad (2.11c) \end{aligned}$$

$$\begin{aligned} \frac{\partial g_4(\mathbf{r};t)}{\partial t} &= -i\Delta\Omega_2 g_4(\mathbf{r};t) - i\chi F(\mathbf{r};t) \left[-\frac{1}{4} g_3(\mathbf{r};t) - \frac{1}{2} g_4(\mathbf{r};t) \right], \\ & \quad (2.11d) \end{aligned}$$

where $F(\mathbf{r}) \equiv Y_0^{(2)}(\theta, \phi)/r^3$, with the time dependence implicitly contained in the random variables r , θ , and ϕ . The components having $\mu=-1$ will evolve according to the same equations except for the reversed signs at their corresponding coefficients [i.e., let $-i \rightarrow +i$ in Eqs. (2.11)]. For the case of identical spins [cf. Eq. (2.2b)], one can add Eqs.

(2.11a) and (2.11b), and Eqs. (2.11c) and (2.11d). If the vector \mathbf{r} is a random function of time, we get the following equations for the two *ensemble-averaged* spin-isochromat components:

$$\begin{aligned} g_+(t) &= \exp(-i\Delta\Omega t) \left\langle \exp_0 \left[-i\frac{3}{4}\chi \int_0^t dt' F(\mathbf{r}(t')) \right] \right\rangle \\ & \quad \times g_+(0), \end{aligned} \quad (2.12a)$$

$$\begin{aligned} g_-(t) &= \exp(-i\Delta\Omega t) \left\langle \exp_0 \left[+i\frac{3}{4}\chi \int_0^t dt' F(\mathbf{r}(t')) \right] \right\rangle \\ & \quad \times g_-(0), \end{aligned} \quad (2.12b)$$

Here $g_+(t) \equiv g_1(t) + g_2(t)$, $g_-(t) \equiv g_3(t) + g_4(t)$, $g_\epsilon(t) \equiv \langle g_\epsilon(\mathbf{r};t) \rangle$. We have written the isochromat components as time-ordered exponentials for the convenient description of their ensemble-averaging to be performed in the next section. In the high-temperature approximation, immediately after a nonselective $\pi/2$ pulse, one has

$$\begin{aligned} \rho(0+) &= -\frac{\hbar\Omega}{4kT} [I_y^{(1)} + I_y^{(2)}] \rightarrow I_+^{(1)} - I_-^{(1)} + I_+^{(2)} - I_-^{(2)} \\ &= E_1 + E_2 + E_3 + E_4 - E_5 - E_6 - E_7 - E_8. \end{aligned} \quad (2.13)$$

The $\mu=\pm 1$ part will yield a component oscillating at $\pm\Delta\Omega$ in the rotating frame. The total FID signal corresponding to $\mu=+1$ can then be written as a sum of the two isochromat components

$$\begin{aligned} G(t) &= g_+(t) + g_-(t) \\ &= q \exp(-i\Delta\Omega t) \left\langle \exp_0 \left[-i\frac{3}{4}\chi \int_0^t dt' F(\mathbf{r}(t')) \right] \right. \\ & \quad \left. + \exp_0 \left[+i\frac{3}{4}\chi \int_0^t dt' F(\mathbf{r}(t')) \right] \right\rangle, \end{aligned} \quad (2.14)$$

where the initial intensities are given by $g_+(0) = g_-(0) = q \equiv i\hbar\Omega/4kT$. The $\mu=-1$ components are related to those with $\mu=+1$ by complex conjugation, since the bracketed part in Eq. (2.14) is real.

III. EVALUATION OF ENSEMBLE-AVERAGED ISOCHROMAT COMPONENTS BY THE STOCHASTIC LIOUVILLE EQUATION (SLE)

The ensemble-averaged ordered exponentials in Eqs. (2.12a) and (2.12b) can be written as⁹

$$\begin{aligned} & \left\langle \exp_0 \left[\mp i\frac{3}{4}\chi \int_0^t dt' F(\mathbf{r}(t')) \right] \right\rangle \\ &= 1 + \sum_{n=1}^{\infty} \left(\mp i\frac{3}{4}\chi \right)^n \int_0^t dt_1 \int_0^{t_1} dt_2 \cdots \int_0^{t_{n-1}} dt_n \\ & \quad \times \int \mathbf{d}^3\mathbf{r}_1 \int \mathbf{d}^3\mathbf{r}_2 \cdots \int \mathbf{d}^3\mathbf{r}_n F(\mathbf{r}_1) F(\mathbf{r}_2) \cdots F(\mathbf{r}_n) \\ & \quad \times p_n(\mathbf{r}_1, t_1; \mathbf{r}_2, t_2; \dots; \mathbf{r}_n, t_n), \end{aligned} \quad (3.1)$$

where $p_n(\mathbf{r}_1, t_1; \mathbf{r}_2, t_2; \dots; \mathbf{r}_n, t_n)$ is the n 'th order joint probability, which for a Markov process is equal to

$$p_n(\mathbf{r}_1, t_1; \mathbf{r}_2, t_2; \dots; \mathbf{r}_n, t_n) = P(\mathbf{r}_1, t_1 | \mathbf{r}_2, t_2) \cdots P(\mathbf{r}_{n-1}, t_{n-1} | \mathbf{r}_n, t_n) p_{\text{eq}}(\mathbf{r}_n, t_n) \quad (3.2)$$

with $p_{\text{eq}}(\mathbf{r}_n, t_n)$ the equilibrium probability density and $P(\mathbf{r}_{n-1}, t_{n-1} | \mathbf{r}_n, t_n)$ the conditional probability that given a spin is at \mathbf{r}_n at time t_n , it will be at \mathbf{r}_{n-1} at t_{n-1} . The isochromat components in Eq. (3.1) can be calculated by solving the SLE^{3,21} for the auxiliary functions $g_{\pm}(\mathbf{r}, t)$ such that

$$\int \mathbf{d}^3 \mathbf{r} g_{\pm}(\mathbf{r}, t) = g_{\pm}(t) = q \exp(-i\Delta\Omega t) \times \left\langle \exp_0 \left[\mp i \frac{3}{4} \chi \int_0^t dt' F(\mathbf{r}(t')) \right] \right\rangle. \quad (3.3)$$

For a stationary Markov process [i.e., $p_{\text{eq}}(\mathbf{r}, t) = p_{\text{eq}}(\mathbf{r})$], the auxiliary function $g_{\pm}(\mathbf{r}, t)$ is formally given in terms of a series expansion

$$g_{\pm}(\mathbf{r}, t) = q \exp(-i\Delta\Omega t) \left[p_{\text{eq}}(\mathbf{r}) + \left(\mp i \frac{3}{4} \chi \right) \int_0^t dt_1 \int \mathbf{d}^3 \mathbf{r}_1 F(\mathbf{r}_1) P(\mathbf{r}, t | \mathbf{r}_1, t_1) p_{\text{eq}}(\mathbf{r}_1) + \left(\mp i \frac{3}{4} \chi \right)^2 \int_0^t dt_1 \int_0^{t_1} dt_2 \int \mathbf{d}^3 \mathbf{r}_1 \int \mathbf{d}^3 \mathbf{r}_2 F(\mathbf{r}_1) F(\mathbf{r}_2) P(\mathbf{r}, t | \mathbf{r}_1, t_1) P(\mathbf{r}_1, t_1 | \mathbf{r}_2, t_2) p_{\text{eq}}(\mathbf{r}_2) + \left(\mp i \frac{3}{4} \chi \right)^3 \int_0^t dt_1 \int_0^{t_1} dt_2 \int_0^{t_2} dt_3 \int \mathbf{d}^3 \mathbf{r}_1 \int \mathbf{d}^3 \mathbf{r}_2 \int \mathbf{d}^3 \mathbf{r}_3 F(\mathbf{r}_1) F(\mathbf{r}_2) F(\mathbf{r}_3) \times P(\mathbf{r}, t | \mathbf{r}_1, t_1) P(\mathbf{r}_1, t_1 | \mathbf{r}_2, t_2) P(\mathbf{r}_2, t_2 | \mathbf{r}_3, t_3) p_{\text{eq}}(\mathbf{r}_3) + \dots \right], \quad (3.4)$$

where the normalized conditional probability $P(\mathbf{r}, t | \mathbf{r}_1, t_1)$ satisfies the equation

$$\frac{\partial P(\mathbf{r}, t | \mathbf{r}_1, t_1)}{\partial t} = \Gamma_{\mathbf{r}} P(\mathbf{r}, t | \mathbf{r}_1, t_1), \quad (3.5)$$

with the initial condition $P(\mathbf{r}, t | \mathbf{r}_1, t_1)|_{t=t_1} = \delta(\mathbf{r} - \mathbf{r}_1)$ and $\Gamma_{\mathbf{r}} p_{\text{eq}}(\mathbf{r}) = 0$. Using the expression for the joint probability for a Markov process, Eq. (3.2), one is able to show that integration of $g_{\pm}(\mathbf{r}, t)$ over \mathbf{r} yields the ensemble-averaged ordered exponential, Eq. (3.1). Then by differentiating Eq. (3.4) with respect to time t , followed by subtracting the result of the action of the operator $\Gamma_{\mathbf{r}}$, using Eq. (3.5) with its conditions, one can show that $g_{\pm}(\mathbf{r}, t)$ satisfies the corresponding SLE

$$\frac{\partial g_{\pm}(\mathbf{r}, t)}{\partial t} = -i[\Delta\Omega \pm i \frac{3}{4} \chi F(\mathbf{r})] g_{\pm}(\mathbf{r}, t) + \Gamma_{\mathbf{r}} g_{\pm}(\mathbf{r}, t). \quad (3.6)$$

Thus, the ensemble-averaged spin-isochromat components are obtained by solving the SLE, Eq. (3.6), followed by integration over \mathbf{r} , cf. Eq. (3.3). Note that Eq. (3.6) is essentially identical to the expression introduced by Kac²² for the purpose of path-averaging exponentials of the type of Eq. (3.1). In addition, the time-ordered structure of $g_{\pm}(\mathbf{r}, t)$ [cf. Eq. (3.4)] allows Eq. (3.6) to be generalized for the case when $F(\mathbf{r})$ is an operator or a superoperator. This leads to a general SLE for the density matrix.^{3,23}

Comparing Eqs. (3.1)–(3.3) we see that we should also require that at $t=0$, $g_{\pm}(\mathbf{r}, t)$ be equal to the equilibrium distribution, viz.

$$g_{\pm}(\mathbf{r}, 0) = q p_{\text{eq}}(\mathbf{r}). \quad (3.7)$$

For convenience in numerical solution, we shall impose the reflecting wall boundary conditions^{12,20}

$$\left. \frac{\partial g_{\pm}(\mathbf{r}, t)}{\partial r} \right|_{r=d} = \left. \frac{\partial g_{\pm}(\mathbf{r}, t)}{\partial r} \right|_{r=r_{\text{max}}} = 0, \quad (3.8)$$

where $d \equiv r_{\text{min}}$ and r_{max} are the distances of the closest approach and the maximum separation between the two spin particles, respectively. Note that if $F(\mathbf{r})$ is a real function, then it follows from Eq. (3.6) that the two FID isochromats are related by complex conjugation, namely

$$g_+(\mathbf{r}, t) e^{i\Delta\Omega t} = g_-^*(\mathbf{r}, t) e^{-i\Delta\Omega t}. \quad (3.9)$$

The total spectral function of two particles of spins 1/2 is calculated by Fourier transforming the spin isochromat components. Eqs. (2.12a) and (2.12b), and is given by

$$\begin{aligned} \tilde{g}_{\text{tot}}(\mathbf{r}, \omega - \Delta\Omega) &\equiv \tilde{g}_+(\mathbf{r}, \omega - \Delta\Omega) + \tilde{g}_-(\mathbf{r}, \omega - \Delta\Omega) \\ &= \tilde{g}_+(\mathbf{r}, \omega - \Delta\Omega) + \tilde{g}_+^*(\mathbf{r}, -\omega + \Delta\Omega). \end{aligned} \quad (3.10)$$

Hence, below we shall just solve for $g_+(\mathbf{r}, t)$ or $g(\mathbf{r}, t)$ and drop the subscript “+” for the FID components.

Let Γ_r now be the translational diffusion operator expressed in spherical polar coordinates, with the diffusion coefficient, D_T . For simplicity, we ignore any other interactions between the two particles. If \mathbf{r} is the relative distance between two identical spin-bearing particles, then D_T becomes twice the diffusion coefficient for the individual particles.¹ By Fourier transforming the SLE, Eq. (3.6), one obtains

$$g(\mathbf{r}, 0) + i\omega \tilde{g}(\mathbf{r}, \omega) + \Gamma_r \tilde{g}(\mathbf{r}, \omega) = i[\Delta\Omega + \frac{3}{4}\chi F(\mathbf{r})] \tilde{g}(\mathbf{r}, \omega). \tag{3.11}$$

We solve Eq. (3.11) by using a spherical harmonic expansion for the angular part of $\tilde{g}(\mathbf{r}, \omega)$, while discretizing the radial part of Γ_r by finite-differences as discussed in Refs. 12 and 20. We look for the solution of Eq. (3.11) in the form

$$\tilde{g}(\mathbf{r}, \omega) = \sum_{l=0}^{\infty} \sum_{m=-l}^l \frac{g_m^{(l)}(r, \omega)}{r} Y_m^{(l)}(\theta, \phi). \tag{3.12}$$

By substituting Eq. (3.12) into Eq. (3.11) and making use of the orthogonality of the spherical harmonics one obtains

$$\begin{aligned} & q\sqrt{4\pi r} \delta_{l,0} \delta_{m,0} + i(\omega - \Delta\Omega) g_m^{(l)}(r, \omega) \\ & + D_T \left[\frac{\partial^2}{\partial r^2} - \frac{l(l+1)}{r^2} \right] g_m^{(l)}(r, \omega) \\ & = i\frac{3}{4}\chi \left[c_m^{(l,l-2)} \frac{g_m^{(l-2)}(r, \omega)}{r^3} + c_m^{(l,l)} \frac{g_m^{(l)}(r, \omega)}{r^3} \right] \end{aligned}$$

$$+ c_m^{(l,l+2)} \frac{g_m^{(l+2)}(r, \omega)}{r^3} \tag{3.13}$$

where we have taken into account the initial condition given by Eq. (3.7), and the coupling coefficients $c_m^{(l,l')}$ are given in terms of the Clebsch–Gordan coefficients

$$\begin{aligned} c_m^{(l,l')} &= \int \sin\theta d\theta d\phi Y_m^{(l)}(\theta, \phi) * Y_0^{(2)}(\theta, \phi) Y_m^{(l')}(\theta, \phi) \\ &= \delta_{m,m'} \sqrt{\frac{5}{4\pi} \frac{(2l'+1)}{(2l+1)}} \langle l'200 | l'2l0 \rangle \\ &\quad \times \langle l'2m'0 | l'2lm \rangle. \end{aligned} \tag{3.14}$$

As can be seen from Eq. (3.13), coefficients with different values of m are uncoupled from each other, and coefficients with even l 's only couple to those with even l 's, and odd l 's only couple to odd l 's. As a result, we just need to consider terms with $m=0$ and l even, since only the term $g_0^{(0)}(\mathbf{r}, \omega)$ is nonzero upon integration over space, cf. Eq. (3.3). Therefore, the line shape problem reduces to the solution of the following block-matrix equation:

$$\begin{pmatrix} -i(\omega - \Delta\Omega)\mathbf{I} + \mathbf{W}_0 & \mathbf{X}_{02} & \mathbf{0} & \mathbf{0} & \dots & \mathbf{0} \\ \mathbf{X}_{20} & -i(\omega - \Delta\Omega)\mathbf{I} + \mathbf{W}_2 & \mathbf{X}_{24} & \mathbf{0} & \dots & \mathbf{0} \\ \mathbf{0} & \mathbf{X}_{42} & -i(\omega - \Delta\Omega)\mathbf{I} + \mathbf{W}_4 & \mathbf{X}_{46} & \dots & \mathbf{0} \\ \mathbf{0} & \mathbf{0} & \mathbf{X}_{64} & -i(\omega - \Delta\Omega)\mathbf{I} + \mathbf{W}_6 & \dots & \mathbf{0} \\ \dots & \dots & \dots & \dots & \dots & \dots \\ \mathbf{0} & \mathbf{0} & \mathbf{0} & \mathbf{0} & \dots & -i(\omega - \Delta\Omega)\mathbf{I} + \mathbf{W}_{L_{\max}} \end{pmatrix} \times \begin{pmatrix} \mathbf{g}^{(0)} \\ \mathbf{g}^{(2)} \\ \mathbf{g}^{(4)} \\ \mathbf{g}^{(6)} \\ \dots \\ \mathbf{g}^{(L_{\max})} \end{pmatrix} = q\sqrt{4\pi} \begin{pmatrix} \mathbf{r} \\ \mathbf{0} \\ \mathbf{0} \\ \mathbf{0} \\ \dots \\ \mathbf{0} \end{pmatrix}. \tag{3.15}$$

Here $\mathbf{0}$ designates a null matrix, \mathbf{I} is a unit matrix, and the size of each block depends on the discretization of the radial part from $r_0=d$ to $r_n=r_{\max}$ with step size Δr . The vector approximating \mathbf{r} is given by $(r_0, r_1, r_2, \dots, r_n)^T$ and $\mathbf{g}^{(l)} = [g^{(l)}(r_0), g^{(l)}(r_1), g^{(l)}(r_2), \dots, g^{(l)}(r_n)]^T$. The index m has been omitted since one is only interested in $g_m^{(l)}(r, \omega)$ with

$m=0$. The matrices $\mathbf{X}_{l,l+2}$ and $\mathbf{X}_{l+2,l}$ are equal as follows from the properties of the Clebsch–Gordan coefficients. The matrices on the diagonal \mathbf{W}_l are obtained by taking into account the boundary conditions, Eq. (3.8) and the condition of the conservation of the overall probability, cf. Ref. 12. We have for \mathbf{W}_l

$$\mathbf{W}_l = \begin{pmatrix} i\frac{3}{4}\chi \frac{c^{(l,l)}}{r_0^3} + \frac{2D_T}{\Delta r^2} \left(1 + \frac{\Delta r}{d}\right) + \frac{D_T l(l+1)}{r_0^2} & -\frac{2D_T}{\Delta r^2} & 0 & \cdots & 0 & 0 \\ -\frac{D_T}{\Delta r^2} & i\frac{3}{4}\chi \frac{c^{(l,l)}}{r_1^3} + \frac{2D_T}{\Delta r^2} + \frac{D_T l(l+1)}{r_1^2} & -\frac{D_T}{\Delta r^2} & \cdots & 0 & 0 \\ 0 & -\frac{D_T}{\Delta r^2} & i\frac{3}{4}\chi \frac{c^{(l,l)}}{r_2^3} + \frac{2D_T}{\Delta r^2} + \frac{D_T l(l+1)}{r_2^2} & \cdots & 0 & 0 \\ \cdots & \cdots & \cdots & \cdots & \cdots & \cdots \\ 0 & 0 & 0 & \cdots & i\frac{3}{4}\chi \frac{c^{(l,l)}}{r_{n-1}^3} + \frac{2D_T}{\Delta r^2} + \frac{D_T l(l+1)}{r_{n-1}^2} & -\frac{D_T}{\Delta r^2} \\ 0 & 0 & 0 & \cdots & -\frac{2D_T}{\Delta r^2} & i\frac{3}{4}\chi \frac{c^{(l,l)}}{r_n^3} + \frac{2D_T}{\Delta r^2} \left(1 - \frac{\Delta r}{d}\right) + \frac{D_T l(l+1)}{r_n^2} \end{pmatrix}. \quad (3.16)$$

Whereas the matrices $\mathbf{X}_{l,l+2}$ are given by

$$\mathbf{X}_{l,l+2} = \begin{pmatrix} i\frac{3}{4}\chi \frac{c^{(l,l+2)}}{r_0^3} & 0 & 0 & \cdots & 0 & 0 \\ 0 & i\frac{3}{4}\chi \frac{c^{(l,l+2)}}{r_1^3} & 0 & \cdots & 0 & 0 \\ 0 & 0 & i\frac{3}{4}\chi \frac{c^{(l,l+2)}}{r_2^3} & \cdots & 0 & 0 \\ \cdots & \cdots & \cdots & \cdots & \cdots & \cdots \\ 0 & 0 & 0 & \cdots & i\frac{3}{4}\chi \frac{c^{(l,l+2)}}{r_{n-1}^3} & 0 \\ 0 & 0 & 0 & \cdots & 0 & i\frac{3}{4}\chi \frac{c^{(l,l+2)}}{r_n^3} \end{pmatrix}. \quad (3.17)$$

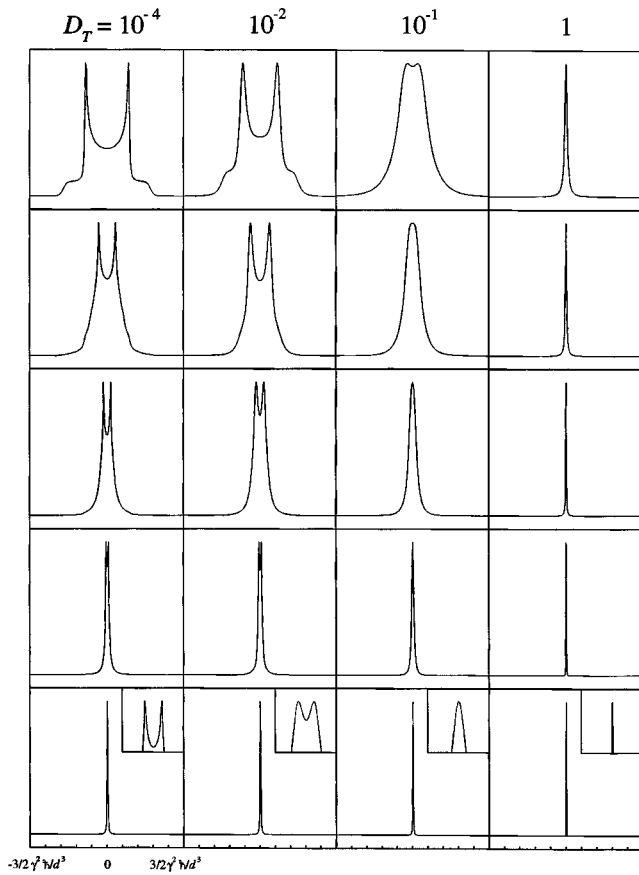


FIG. 1. Modulation of dipolar line shapes by translational diffusion for two spins of 1/2. Line shapes are simulated as a function of the diffusion coefficient D_T (in units of $\gamma^2\hbar/d$) and the ratio of the maximum separation with respect to the distance of minimal approach, r_{\max}/d for values of 1.1, 1.5, 2, and 5 from top to bottom. The values for D_T and r_{\max}/d are chosen as indicated. Equation (2.14) has been used, evaluated by the stochastic Liouville equation method, Eq. (3.6). The entire motional range from classical Pake patterns to motionally narrowed Lorentzians is recovered. For the value $r_{\max}/d=5$, magnified insets (~ 50 times in each linear dimension) are included to show that dipolar doublets collapse at lower values of D_T in comparison with pure rotation, i.e., when $r_{\max}/d \approx 1$. Note that the abscissa corresponds to units of angular frequency (i.e., ω) from $-\frac{3}{2}\gamma^2\hbar/d^3$ to $+\frac{3}{2}\gamma^2\hbar/d^3$ in all cases.

Coefficients $g_m^{(l)}(r, \omega)$ can then be found by numerically inverting the block-matrix equation. The spectrum can be computed by using Eq. (3.12) followed by integration over \mathbf{r} , yielding:

$$\begin{aligned} \tilde{g}(\omega) &= \int \mathbf{d}^3\mathbf{r} \tilde{g}(\mathbf{r}, \omega) \\ &= \sum_{l=0}^{\infty} \sum_{m=-l}^l \int \sin\theta d\theta d\phi \int r^2 dr \frac{g_m^{(l)}(r, \omega)}{r} Y_m^{(l)}(\theta, \phi) \\ &= \sqrt{4\pi} \int r dr g_0^{(0)}(r, \omega). \end{aligned} \quad (3.18)$$

Calculated spectra are plotted in Fig. 1 for different values of the diffusion coefficient D_T and ratio r_{\max}/d . In order to converge and to obtain a smooth spectrum, several hundred points are sufficient for the discretization of r -space; whereas the value of L_{\max} can be kept at around 20.

IV. EVOLUTION OF ISOCROMAT COMPONENTS IN THE CASE OF ADDITIONAL PULSES

We have discussed so far the case of the cw (continuous wave) spectrum, or alternatively the FID modulation by the dipolar interaction. We now extend the eigenoperator expansion method for additional pulses (cf. Refs. 24 and 25 for an alternative approach). Since it is well-known that a π -pulse will not refocus the dipolar interaction, let us consider a solid-echo experiment,² which involves a second pulse $(\pi/2)_y$ that is applied along the rotating y axis at time τ . If the pulse is nonselective, the eigenoperators having $\mu=1$ involved in the density matrix expansion, cf. Eq. (2.10), will be transformed by the pulse action as

$$I_+^{(1)} I_\alpha^{(2)} \rightarrow \frac{1}{4} [I_\alpha^{(1)} - I_\beta^{(1)} + I_+^{(1)} - I_-^{(1)}] [I_\alpha^{(2)} + I_\beta^{(2)} - I_+^{(2)} - I_-^{(2)}], \quad (4.1a)$$

$$I_+^{(1)} I_\beta^{(2)} \rightarrow \frac{1}{4} [I_\alpha^{(1)} - I_\beta^{(1)} + I_+^{(1)} - I_-^{(1)}] [I_\alpha^{(2)} + I_\beta^{(2)} + I_+^{(2)} + I_-^{(2)}], \quad (4.1b)$$

plus the permutation of indices 1 and 2. Here we have used the relations: $I_\alpha - I_\beta = 2I_z$ and $I_\alpha + I_\beta = 1$. From Eqs. (4.1a) and (4.1b) one can easily obtain the corresponding relations for operators having $\mu=-1$. Moreover, one can see from Eqs. (4.1a) and (4.1b), the additional $(\pi/2)_y$ pulse mixes the components $g_\epsilon(\mathbf{r}; t)$ having $\mu=1$ with those having $\mu=-1$. If the system is on resonance, i.e., $\Delta\Omega=0$, it is well-known² that the components with $\mu=0, \pm 2$ corresponding to zero and double quantum coherences, will not be excited by the second pulse. Thus, in order to calculate the solid-echo signal it is sufficient to consider the eigenoperator subspace with $\mu=\pm 1$. To describe the effect of a hard or nonselective pulse we introduce a pulse propagator matrix \mathbf{X} , which transforms the eigenoperators E_ϵ , $\epsilon=1, \dots, 8$ according to Eqs. (4.1a) and (4.1b), and relates the ‘‘vector’’ consisting of coefficients of the density matrix expansion, Eq. (2.10), before and immediately after the pulse

$$\mathbf{g}(\mathbf{r}; \tau+) = \mathbf{X}\mathbf{g}(\mathbf{r}; \tau). \quad (4.2)$$

Calculation of the elements of the matrix \mathbf{X} from Eqs. (4.1a) and (4.1b) yields

$$\mathbf{X} = \frac{1}{4} \begin{pmatrix} 1 & -1 & 1 & 1 & -1 & -1 & -1 & 1 \\ -1 & 1 & 1 & 1 & -1 & -1 & 1 & -1 \\ 1 & 1 & 1 & -1 & -1 & 1 & -1 & -1 \\ 1 & 1 & -1 & 1 & 1 & -1 & -1 & -1 \\ -1 & -1 & -1 & 1 & 1 & -1 & 1 & 1 \\ -1 & -1 & 1 & -1 & -1 & 1 & 1 & 1 \\ -1 & 1 & -1 & -1 & 1 & 1 & 1 & -1 \\ 1 & -1 & -1 & -1 & 1 & 1 & -1 & 1 \end{pmatrix}. \quad (4.3)$$

Here the elements of the matrix \mathbf{X} are arranged according to $\epsilon=1, \dots, 8$. Note that Eq. (4.3) represents only the part of the full matrix \mathbf{X} corresponding to $\mu=\pm 1$ which is needed to calculate the observed signal.

The vector-coefficient $\mathbf{g}(\mathbf{r}; \tau)$ at time τ just before the pulse can be written by formally resolving Eqs. (2.11)

$$\mathbf{g}(\mathbf{r}; \tau) = e^{-i\Delta\Omega\tau} e^{-i\chi\mathbf{C}\int_0^\tau dt' F(\mathbf{r}(t'))} \mathbf{g}(0), \quad (4.4)$$

where the initial magnetization vector is given by: $\mathbf{g}(0) = q(1, 1, 1, 1, -1, -1, -1, -1)^T$ since after the first $(\pi/2)_x$ pulse the magnetization is along the rotating y axis, and $I_y = (I_+ - I_-)/2i$. The dipolar interaction matrix \mathbf{C} is obtained from Eqs. (2.11a)–(2.11d) as well as from the equivalent equations for the case of $\mu = -1$. It represents the numerical coefficients of $g_\epsilon(\mathbf{r}; t)$ in these equations. In the basis of eigenoperators E_ϵ , $\epsilon = 1, 2, \dots, 8$, the \mathbf{C} -matrix is equal to²⁶

$$\mathbf{C} = \begin{pmatrix} \frac{1}{2} & \frac{1}{4} & & & & & & \\ & \frac{1}{4} & \frac{1}{2} & & & & & \\ & & -\frac{1}{2} & -\frac{1}{4} & & & & \\ & & -\frac{1}{4} & -\frac{1}{2} & & & & \\ & & & & -\frac{1}{2} & -\frac{1}{4} & & \\ & & & & -\frac{1}{4} & -\frac{1}{2} & & \\ & & & & & & \frac{1}{2} & \frac{1}{4} \\ & & & & & & \frac{1}{4} & \frac{1}{2} \end{pmatrix}. \quad (4.5)$$

The matrix of frequency offsets, $\Delta\Omega$ is also obtained from Eqs. (2.11) and the associated equations for $\mu = -1$, and is equal to

$$\Delta\Omega = \begin{pmatrix} (\Omega - \omega_{rf})\mathbf{I} & \mathbf{0} \\ \mathbf{0} & -(\Omega - \omega_{rf})\mathbf{I} \end{pmatrix}, \quad (4.6)$$

where \mathbf{I} designates the 4 by 4 unit matrix, $\mathbf{0}$ is the 4 by 4 null matrix.

Finally, using Eqs. (4.2) and (4.4), the overall vector of the *ensemble-averaged* components $\mathbf{g}(t)$ in the rotating frame at times $t > \tau$ can be represented by the following equation:

$$\mathbf{g}(t) = \langle \mathbf{g}(\mathbf{r}; t) \rangle = \langle e^{-i\Delta\Omega(t-\tau)} e^{-i\chi\mathbf{C}\int_\tau^t dt' F(\mathbf{r}(t'))} \times \mathbf{X} e^{-i\Delta\Omega\tau} e^{-i\chi\mathbf{C}\int_0^\tau dt' F(\mathbf{r}(t'))} \rangle \mathbf{g}(0). \quad (4.7)$$

We shall further consider the on-resonance case when $\Delta\Omega = \mathbf{0}$. If we were to let $\Delta\Omega \neq \mathbf{0}$, then coherences with $\mu = 0, \pm 2$ would also be excited, thereby requiring the full 16×16 matrix forms of \mathbf{C} , $\Delta\Omega$, and \mathbf{X} . One sees from the structure of \mathbf{C} given by Eq. (4.5), consisting of 2×2 blocks, that each consecutive pair of elements in the starting vector $\mathbf{g}(0)$ forms an eigenvector of the corresponding block of the matrix \mathbf{C} with eigenvalues $\pm 3/4$. This fact greatly simplifies the calculations of the matrix exponentials. Performing the necessary matrix multiplication and summing over the components of $\mathbf{g}(t)$ having $\mu = 1$, one obtains [cf. Eqs. (2.5) and (2.14)]

$$\begin{aligned} G(t) &= q \left\langle \exp_0 \left[-i\frac{3}{4}\chi \int_\tau^t dt' F(\mathbf{r}(t')) + i\frac{3}{4}\chi \int_0^\tau dt' F(\mathbf{r}(t')) \right] \right. \\ &\quad \left. + \exp_0 \left[+i\frac{3}{4}\chi \int_\tau^t dt' F(\mathbf{r}(t')) - i\frac{3}{4}\chi \int_0^\tau dt' F(\mathbf{r}(t')) \right] \right\rangle \\ &= q \left\langle \exp_0 \left[-i\frac{3}{4}\chi \int_0^t dt' s(t') F(\mathbf{r}(t')) \right] \right. \\ &\quad \left. + \exp_0 \left[+i\frac{3}{4}\chi \int_0^t dt' s(t') F(\mathbf{r}(t')) \right] \right\rangle, \quad (4.8) \end{aligned}$$

where we have introduced the pulse function $s(t)$, such that $s(t) = +1$ if $t > \tau$ and $s(t) = -1$ if $0 < t < \tau$. It should be noted that the ensemble-averaged isochromat components in Eq. (4.8) are analogous to the phase functions introduced by Klauder and Anderson.²⁷ Here, they arise naturally as a direct consequence of the transformation of the symmetry-adapted eigenoperator basis in a pulse sequence, which determines the specific form of $s(t)$. If one were off-resonance, an additional factor of $\cos(\Delta\Omega\tau)$ would appear in front of Eq. (4.8), representing oscillations between the first-order coherence, and the zeroth- and second-order coherences.

The spin-isochromat components in the presence of pulses of the type used in the solid echo can be evaluated in terms of a modified SLE by analogy with the FID components of Eq. (2.14) upon replacing the function $F(\mathbf{r}(t))$ with $s(t)F(\mathbf{r}(t))$ in Eq. (3.1) (cf. Ref. 24 for an alternative approach). Constructing a formal series expansion for the auxiliary function $g_\pm(\mathbf{r}, t)$, cf. Eq. (3.4), it can be shown that the latter satisfies a modified stochastic Liouville equation, viz.

$$\frac{\partial g_\pm(\mathbf{r}, t)}{\partial t} - \Gamma_r g_\pm(\mathbf{r}, t) = \mp i\frac{3}{4}\chi F(\mathbf{r}) s(t) g_\pm(\mathbf{r}, t). \quad (4.9)$$

Note that for a $(\pi/2)_y$ pulse at $t = \tau$, for the spin Hamiltonian of Eqs. (2.1)–(2.3), the stochastic Liouville operator at $t > \tau$ and the operator at $0 < t < \tau$ are related by complex conjugation. Therefore, the overall solution at $t > \tau$ can be written in operator form as

$$g_\pm(\mathbf{r}, t) = \exp[L_\pm(t - \tau)] \exp[L_\pm^* \tau] g_\pm(\mathbf{r}, 0), \quad (4.10)$$

where $L_\pm \equiv \Gamma_r \mp i\frac{3}{4}\chi F(\mathbf{r})$ is the stochastic Liouville operator. Equation (4.10) can be solved in the time domain by first finding the eigenvalues and eigenvectors of the stochastic Liouville operator in the matrix representation described in Sec. III. It is convenient here to use a form of the Lanczos algorithm appropriate for complex *nonsymmetric matrices*.^{5,28,29} We actually used, for calculations, the standard MATLAB (MathWorks, Inc.) package implementing the Arnoldi method, which is closely related to the Lanczos method.³⁰

V. SPECTRAL LINE SHAPES AND ECHO AMPLITUDES IN THE PRESENCE OF TRANSLATIONAL DIFFUSION

Cw signals from two particles of spin 1/2 which diffuse relative to each other, obtained from the Fourier transform of Eq. (2.14) using the method of Sec. III, are presented in Fig. 1. The motion of the spin pair is characterized by the coef-

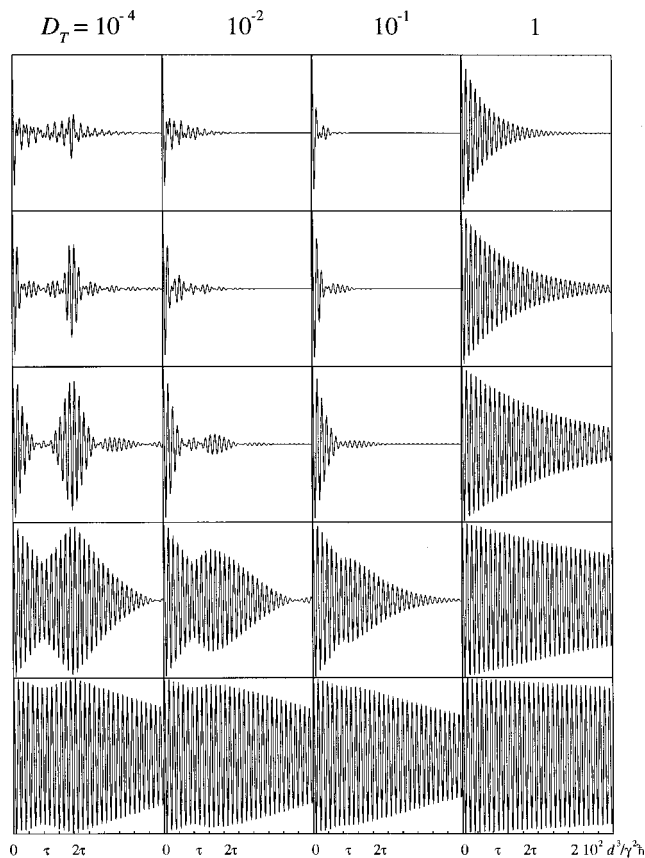


FIG. 2. Simulation of solid echoes for two spins of 1/2 as a function of the diffusion coefficient D_T (in units of $\gamma^2\hbar/d$) and the ratio of the maximum separation to the distance of minimal approach, r_{\max}/d for values of 1.1, 1.5, 2, 3, and 5 from top to bottom. The echo signal is calculated by using Eq. (4.10) integrated over volume as implied by Eq. (4.8). The second $(\pi/2)_y$ pulse is applied at time τ as indicated. Apparent similarity between the motionally narrowed Lorentzians and the line shapes narrowed by increasing the ratio r_{\max}/d , cf. Fig. 1, is removed by refocusing the inhomogeneous line broadening in the latter case; whereas at higher motional rates line broadening is homogeneous and cannot be refocused.

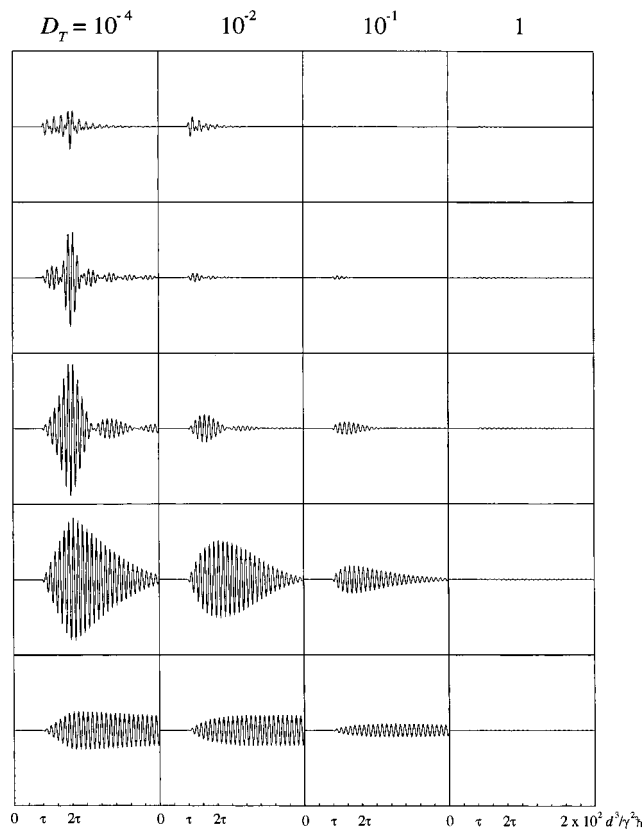


FIG. 3. The FID signal has been subtracted here from the solid-echo signal (cf. Fig. 2) thereby showing pure echoes and secondary echoes. No appreciable echo signal is observed at fast motions, where line broadening is homogeneous. Increasing the ratio r_{\max}/d yields greater residual signal, which is clearly seen in the intermediate motional regime. The amplitude of the refocused signal first grows with r_{\max}/d , and then decreases. The echo maximum shifts with D_T , and does not always occur at 2τ , except for very slow motions. The abscissa and values of r_{\max}/d are as in Fig. 2.

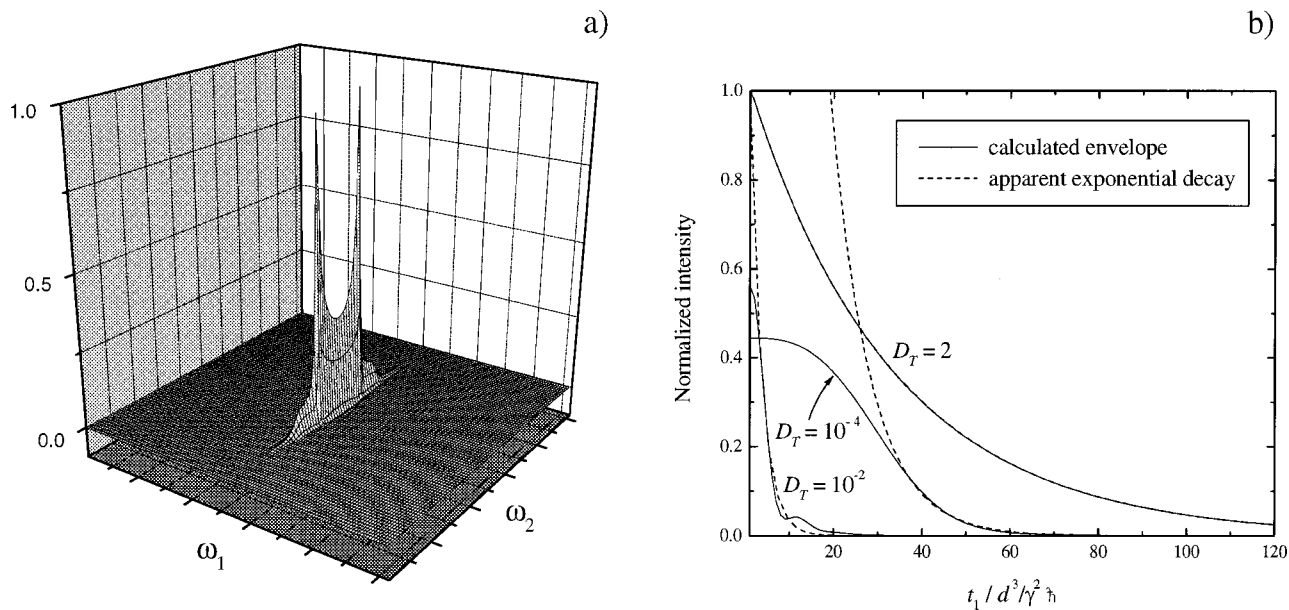


FIG. 4. (a) Illustrative SECSY spectrum for two interacting spin dipoles of 1/2. The spectrum is calculated for $r_{\max}/d=1.1$ and $D_T=10^{-4}$. Horizontal axes correspond to the frequency range of $\pm 2\gamma^2\hbar/d^3$. (b) Echo envelopes vs t_1 for the $\omega_2=0$ slice showing exponential fits used to estimate homogeneous T_2 's.

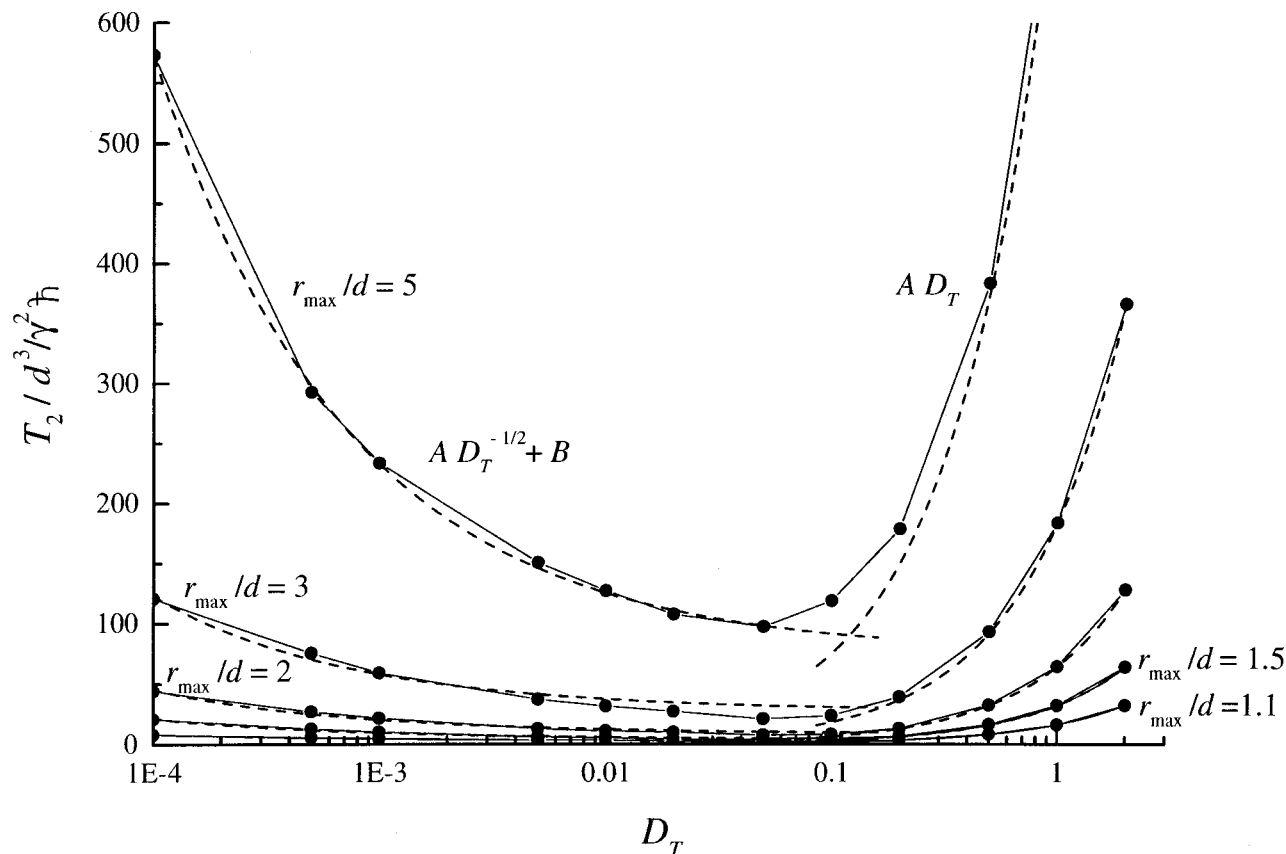


FIG. 5. Homogeneous transverse relaxation times, T_2 , as a function of the diffusion coefficient, D_T , plotted for different values of the ratio of the maximum separation to the distance of minimal approach, r_{\max}/d . The T_2 values are obtained as illustrated in Fig. 4. Distinct T_2 minima are observed at about $D_T = 0.05 \gamma^2 \hbar/d$. Increasing r_{\max}/d does not shift the position of the minimum, implying that the transition to the motional narrowing regime is not affected by the distance of separation between the spins. Limiting behavior (given by the forms $AD_T^{-1/2} + B$ and AD_T) is shown by dashed lines. In the fast motional regime the line broadening is homogeneous and is directly proportional to D_T , i.e., as given by the motional narrowing theory.

efficient D_T for their relative diffusion, the distance of their closest approach d , and their maximum separation r_{\max} . The line shape may be described as a function of two dimensionless parameters: $D_T/d^2\chi$ and r_{\max}/d , cf. Eq. (3.11). For simplicity we have converted to dimensionless units by setting $d=1$, $\gamma^2\hbar/d^3=1$. In this system of units the diffusion coefficient D_T must be multiplied by $\gamma^2\hbar/d$ to obtain its actual value; (in the case of electron spins on molecules for which the distance of closest approach between their centers is $d=10 \text{ \AA}$, this coefficient is equal to $3.27 \times 10^{-6} \text{ cm}^2 \text{ s}^{-1}$; for two protons it is $7.55 \times 10^{-12} \text{ cm}^2 \text{ s}^{-1}$).

As can be seen in Fig. 1, at low values of D_T the line shape consists of two distinct isochromats which merge as D_T increases, finally yielding a Lorentzian line shape corresponding to the motional narrowing regime. If r_{\max}/d is close to unity, the line shape is that of the broad classic dipolar Pake powder pattern. By contrast, increasing the value of r_{\max}/d narrows the spectra as a result of the reduced influence of the dipolar interaction, since on average the two particles become more separated. As the ratio r_{\max}/d becomes larger, Lorentzian line shapes are obtained at smaller values of the diffusion coefficient D_T in comparison with pure rotational diffusion, i.e., when $r_{\max}/d \approx 1$. However, near the rigid limit ($D_T \approx 10^{-4}$) the two isochromats can still be resolved upon magnifying the frequency scale by about 50 times (insets). Given the greatly reduced widths as r_{\max} is

increased, it was not practical to show results for $r_{\max}/d > 5$.

Figure 2 shows simulations of the solid-echo signals for various D_T and ratios r_{\max}/d . To obtain these results, Eq. (4.10) has been used followed by averaging over \mathbf{r} . The $(\pi/2)_y$ pulse is applied at time $\tau = 20 d^3/\gamma^2\hbar$ in all cases. Figure 2 shows both FID-like and echolike behavior obtained from a single expression. Even though some spectra look the same when plotted vs frequency, cf. Fig. 1, the corresponding echo signals allow one to unequivocally distinguish them according to the motional rate of spins D_T and their allowed separation r_{\max} . As can be seen, increasing the rate of the motion yields a decay of the echo amplitudes. In the motional-narrowing regime, $D_T \geq 1$, line broadening is completely homogeneous, hence the signal decay is not affected at all by the refocusing pulse. The decay rates given by T_2^{-1} decrease as r_{\max}/d increases, which is expected, since the effective dipolar interaction is reduced. Echo formation at 2τ is most clearly seen for very slow motions ($D_T \approx 10^{-4}$) where the broadening is mostly inhomogeneous. Moreover, the echo formation is clearest for intermediate values of r_{\max}/d . For smaller values the sharpness of the Pake doublets seen in the spectrum (cf. Fig. 1) interferes with this, and for larger values of r_{\max}/d the dephasing from $0 < t < \tau$ is slow due to smaller effective dipolar interaction. As the motional rate increases, the refocused echo at 2τ is

reduced in magnitude due to the development of a finite homogeneous T_2^{-1} . In order to better isolate these various effects we next show figures that (i) display only the echo-like effect and also (ii) track the homogeneous T_2^{-1} as D_T is varied.

Figure 3 shows the result of subtraction of the FID signals from the signals in Fig. 2 obtained using the solid-echo pulse sequence. Near the rigid limit, one observes a clear echo formation occurring at a time equal to exactly twice the time of the second pulse. As the ratio r_{\max}/d increases, the echo decay times become longer, as already noted. As the diffusion rate increases (e.g., $D_T \approx 10^{-2}$) the echo maximum shifts towards longer times with greater r_{\max}/d . Further increase in D_T yields a decrease in the amplitude of the echo, which vanishes completely in the motional-narrowing limit. Next, the T_2 values have been obtained from simulating the SECSY (spin echo correlation spectroscopy)^{25,31–33} two-dimensional spectra, Fig. 4(a), by using Eqs. (4.8) and (4.10). Here, the t_1 axis corresponds to twice the delay time τ between the first and second pulses in the solid-echo experiment, and the t_2 axis is the acquisition time starting immediately after 2τ , i.e., $t_2 = t - 2\tau$. After a Fourier transformation with respect to t_2 , the zero-frequency ($\omega = 0$) amplitudes have been measured as a function of t_1 . When motions are slow, the early time behavior follows a t_1^3 dependence; whereas the longer time behavior is usually reasonably approximated by a single exponential, consistent with what was previously found for rotational modulation cases²⁴ [cf. Fig. 4(b)]. The T_2 values were determined from single-exponential fits to the longer t_1 behavior (cf. Ref 24). The homogeneous T_2 's as a function of the diffusion coefficient D_T are plotted in Fig. 5. Distinct T_2 minima are observed near $D_T = 0.05$. Allowing the two spins to move farther apart from each other does not shift the position of the minimum, but influences the relative T_2 values as we have already noted above. Note that at higher values of D_T the behavior of T_2 is linear with respect to D_T , i.e., as predicted by motional narrowing theory; whereas a $D_T^{-1/2}$ dependence is observed in the slow motional regime.²⁴

Similar values of the T_2 minima for a range of values of r_{\max}/d suggests that the range of validity of motional narrowing is hardly affected by the value of r_{\max} . This may not be so surprising in view of the fact that whereas the dipolar interaction decreases as χ/r^3 , its effective averaging by pseudo-rotation (i.e., modulation of the orientation of \mathbf{r}) occurs at the rate of D_T/r^2 , thus contributing to the homogeneous T_2 's.

VI. CONCLUSIONS

In the present work, dipolar line shapes (and FID's) for two identical spins of 1/2 have been calculated over the complete range of relative translational motion by decomposing the relevant or detectable part of the spin density matrix into a symmetry-adapted eigenoperator set, which yields the observable signal as a sum of two ensemble-averaged spin isochromats. The latter are then evaluated in terms of appropriate stochastic Liouville equations, in which the spin degrees of freedom are separated from the dynamics of \mathbf{r} , the vector

representing the relative positions of the two spins. This approach was extended to spin echoes, in particular the solid echo sequence, which refocuses the dipolar interaction. This methodology will be seen to enable convenient generalization to the many-body case in Paper II. In the present case one observes line shapes that range from familiar Pake doublets in the rigid limit to motionally averaged Lorentzians in the fast motional regime. Under conditions of motional narrowing the T_2 obeys the usual linear dependence upon D_T , whereas in the slow motional limit the homogeneous T_2 is found to vary as $D_T^{-1/2}$. In this work \mathbf{r} was restricted to a maximum magnitude, r_{\max} , in order to obtain finite values of T_2 . Increasing r_{\max} enabled the diffusion to average the Pake doublets somewhat more effectively, whereas T_2 shows a minimum vs D_T that occurs at about $D_T = 0.05$ (in units of $\gamma^2 \hbar / d^3$), a value that appears to be insensitive to r_{\max} .

The results of this paper can probably best be used to study dipolar interactions between flexible biradicals, as mentioned in Sec. I. In the relevant case of nitroxide biradicals in ESR experiments, one would need to add the corresponding hyperfine interactions of each nitroxide electron spin with the ^{14}N or ^{15}N nuclear spin. Whereas this makes the analysis more complicated in spin-Liouville space,^{3,5} it is otherwise a straightforward application of the methods described in this paper.

ACKNOWLEDGMENTS

We thank Dr. Peter P. Borbat, Dr. Keith A. Earle, and Dr. David J. Schneider, and Professor David B. Zax for insightful discussions. This work was supported by grants from the NSF and the NIH.

- ¹A. Abragam, *The Principles of Nuclear Magnetism* (Oxford University Press, London, 1961).
- ²C. P. Slichter, *Principles of Magnetic Resonance*, 3rd ed. (Springer-Verlag, Heidelberg, 1990).
- ³J. H. Freed, in *Electron Spin Relaxation in Liquids*, edited by L. T. Muus and P. W. Atkins (Plenum, New York, 1972), pp. 387–410.
- ⁴J. H. Freed and J. B. Pedersen, *Adv. Magn. Reson.* **8**, 1 (1976).
- ⁵D. J. Schneider and J. H. Freed, *Adv. Chem. Phys.* **73**, 387 (1989).
- ⁶N. P. Benetis, D. J. Schneider, and J. H. Freed, *J. Magn. Reson.* **85**, 275 (1989).
- ⁷K. M. Salikhov, Y. N. Molin, R. Z. Sagdeev, and A. L. Buchachenko, *Spin Polarization and Magnetic Effects in Radical Interactions* (Elsevier, Amsterdam, 1984).
- ⁸R. Kubo, *J. Phys. Soc. Jpn.* **17**, 1100 (1962).
- ⁹J. H. Freed, *J. Chem. Phys.* **49**, 376 (1968).
- ¹⁰R. Brüschweiler, *J. Prog. Nucl. Magn. Reson. Spectrosc.* **32**, 1 (1998).
- ¹¹H. C. Torrey, *Phys. Rev.* **92**, 962 (1953).
- ¹²L. P. Hwang and J. H. Freed, *J. Chem. Phys.* **63**, 4017 (1975).
- ¹³J. H. Freed, *J. Chem. Phys.* **68**, 4034 (1978).
- ¹⁴A. A. Nevzorov and J. H. Freed, *J. Chem. Phys.* **112**, 1425 (2000), following paper.
- ¹⁵F. J. J. de Kanter, J. A. den Hollander, A. H. Huizer, and R. Kaptein, *Mol. Phys.* **34**, 857 (1977); S. Stob, J. Kemmink, and R. Kaptein, *J. Am. Chem. Soc.* **111**, 7036 (1989).
- ¹⁶M. D. E. Forbes and S. R. Ruberu, *J. Phys. Chem.* **97**, 13223 (1993).
- ¹⁷E. J. Hustedt and A. H. Beth, *Annu. Rev. Biophys. Biomol. Struct.* **28**, 129 (1999).
- ¹⁸V. Pfannebecker, H. Klos, M. Hubrich, T. Volkmer, A. Heuer, U. Wiesner, and H. W. Spiess, *J. Phys. Chem.* **100**, 13428 (1996).
- ¹⁹C. N. Banwell and H. Primas, *Mol. Phys.* **6**, 225 (1963).
- ²⁰G. P. Zientara and J. H. Freed, *J. Phys. Chem.* **83**, 3333 (1979).
- ²¹J. B. Pedersen, in *Electron Spin Relaxation in Liquids*, edited by L. T.

Muus and P. W. Atkins (Plenum, New York, 1972), pp. 25–70.

²²M. Kac, *Probability and Related Topics in Physical Sciences* (Interscience, New York, 1959).

²³R. Kubo, *J. Phys. Soc. Jpn. Suppl.* **26**, 1 (1969).

²⁴L. J. Schwartz, A. E. Stillman, and J. H. Freed, *J. Chem. Phys.* **77**, 5410 (1982).

²⁵S. Lee, D. E. Budil, and J. H. Freed, *J. Chem. Phys.* **101**, 5529 (1994).

²⁶It is easy to find the corresponding form for the C -matrix in the case of Heisenberg exchange. The exchange interaction Hamiltonian is given by:

$$H_J^{(1,2)} = J\mathbf{I}^{(1)} \cdot \mathbf{I}^{(2)} = J \left[I_z^{(1)} I_z^{(2)} + \frac{I_+^{(1)} I_-^{(2)} + I_-^{(1)} I_+^{(2)}}{2} \right].$$

Computing the commutators with the eigenoperators E_ϵ , we have for the elements of the C -matrix:

$$\mathbf{C} = \begin{pmatrix} \pm 1/2 & \mp 1/2 \\ \mp 1/2 & \pm 1/2 \end{pmatrix}.$$

For a nonselective initial pulse, the starting vector $\mathbf{g}(0+) = (1,1)^T$ will yield zero eigenvalues upon multiplication by the matrix \mathbf{C} , thus not affecting the spectrum. This is a well-known result for two identical spins;

when the two spins become distinguishable, then significant effects are found [J. H. Freed, *J. Chem. Phys.* **45**, 3452 (1966)].

²⁷J. R. Klauder and P. W. Anderson, *Phys. Rev.* **125**, 912 (1962).

²⁸J. K. Cullum and R. A. Willoughby, in *Large Scale Eigenvalue Problems*, edited by J. K. Cullum and R. A. Willoughby (North-Holland, Amsterdam, 1986), pp. 193–240.

²⁹G. Moro and J. H. Freed, in *Large Scale Eigenvalue Problems*, edited by J. K. Cullum and R. A. Willoughby (North-Holland, Amsterdam, 1986), pp. 143–161.

³⁰G. H. Golub and F. V. van Loan, *Matrix Computations* (The Johns Hopkins University Press, Baltimore, 1989).

³¹R. R. Ernst, G. Bodenhausen, and A. Wokaun, *Principles of Nuclear Magnetic Resonance in One and Two Dimensions* (Oxford University Press, Oxford, 1987).

³²J. Gorcester, G. L. Millhauser, and J. H. Freed, in *Advanced EPR: Applications in Biology and Biochemistry*, edited by A. J. Hoff (Elsevier, Amsterdam, 1989), Chap. 5, pp. 177–242.

³³J. Gorcester, G. L. Millhauser, and J. H. Freed, in *Modern Pulsed and Continuous-wave Electron Spin Resonance*, edited by L. Kevan and M. Bowman (Wiley, New York, 1990), pp. 119–194.